(4) Wilson, T.; Landis, M. E.; Baumstark, A. M.; Bartlett, P. D. *J. Am. Chem. Soc.* **1973**, *95*, 4765.
(5) (a) T. Wilson in "Chemical Kinetics", Herschbach, D. R., Ed.; Butterworths: London, 1976; p 298. (b) Turro, N. J.; Lechtken, P.; Schuster, G.; Orell, J.; Steinmetzer, H. C.; Adam. W. *J. Am. Chem. Soc.* **1974**, *96*, 1627.
(6) Foote, C. S.; Peters, J. W. *Int. Cong. Pure Appl. Chem., 23rd, 1979, Spec. Lect.* **1979**, *4*, 129.
(7) Bartlett, P. D.; Lahav, M. *Isr. J. Chem.* **1972**, *10*, 10.
(8) Foote, C. S.; Peters, J. W. *J. Am. Chem. Soc.* **1971**, *93*, 3795.
(9) (a) Chapman, O. L.; King, R. W. *J. Am. Chem. Soc.* **1964**, *86*, 1256. (b) McGreer, D. E.; Mocek, M. M. *J. Chem. Educ.* **1963**, *40*, 359.
(10) Leavitt, F.; Levey, M.; Szwarc, M. *J. Am. Chem. Soc.* **1955**, *77*, 5493.
(11) Vasil'ev, R. F. *Prog. React. Kinet.* **1967**, *4*, 317–325, and references cited therein.
(12) Martin, J. C.; Arhart, R. J. *J. Am. Chem. Soc.* **1971**, *93*, 2341.
(13) Arhart, R. J.; Martin, J. C. *J. Am. Chem. Soc.* **1972**, *94*, 5003.
(14) Martin, J. C.; Arhart, R. J.; Franz, J. A.; Perozzi, E. F.; Kaplan, L. J. *Org. Synth.* **1977**, *57*, 22–26.
(15) Rust, F. F.; Seubold, F. H., Jr.; Vaughan, W. E. *J. Am. Chem. Soc.* **1950**, *72*, 338.

Conformational Effects in the Fluorescence and Photochemistry of [2.*n*](9,10)Anthracenophanes (*n* = 4, 5)

Albert Dunand, James Ferguson,* Miroslav Puza, and Glen B. Robertson

Contribution from the Research School of Chemistry, The Australian National University, Canberra, A.C.T. 2600, Australia. *Received June 22, 1979*

Abstract: A molecular force field model has been used to predict the number of possible conformations of [2.4](9,10)anthracenophane (I) and [2.5](9,10)anthracenophane (II). The model predicts four conformers for I and six for II. Calculated heats of formation and observed X-ray structure data provide the most likely conformational arrangements of I and II in their ground states. These have the largest mean interchromophore separations. Absorption of light can lead to excited state intramolecular relaxation in which this separation is reduced. For I there are two recognizable relaxation paths. In the first, there is a relative translation of the two chromophores, in opposite directions, parallel to the long axis of the molecule. This leads to a reduction of fluorescence yield (to 0.68) and a reduction of decay time (to 63 ns) as well as a small red shift of the fluorescence band. In the second, there is a change of conformation of the butane bridge which brings the two chromophores closer together. It is accompanied by an activation barrier of 8.3 kcal mol^{-1} and the new conformation has a fluorescence band with a large red shift. Photochemistry proceeds via this conformation with the formation of the photoisomer. The likely structure of this molecule has an arrangement of the butane bridge which has been found in the crystal structure of the photoisomer of 1,4-di(9-anthryl)butane. For II, the properties of the fluorescence can be rationalized on the basis of only two conformations, each with the same conformation of the pentane bridge. No photochemistry could be observed and no red-shifted fluorescence band, analogous to that of I, was found. Two rotational barriers would be involved to reach the conformation of the pentane bridge in the most likely molecular structure of the photoisomer and the rate is too low to be measurable.

Introduction

The [2.*n*](9,10)anthracenophanes provide a particularly useful series of linked anthracene chromophores. The ethane bridge, common to the series, acts as a hinge permitting the chromophores to open away from the most constrained conformation as the length of the second bridge is increased from *n* = 2. For the latter molecule there exist two crystalline polytypes. In the β form, crystal-structure analysis[1] shows that the arrangement of the two chromophores involves a small relative translation of one chromophore over the other in a direction parallel to the long axis of the molecule. Similar analyses of [2.4](9,10)anthracenophane (I) and [2.5]-(9,10)anthracenophane (II) have been carried out in this laboratory.[2]

I crystallizes in the monoclinic space group $P2_1/c$ with four molecules per unit cell of dimensions a = 10.551 (1) Å, b = 26.512 (3) Å, c = 8.952 (1) Å, and β = 114.735 (8)°. The structure has been refined to a conventional R factor of 0.041 for 2178 observable data. The model obtained exhibits large thermal parameters and some discrepancies in the molecular geometry, characteristic of a disordered structure. It results from the superposition of two molecular conformations which differ (mainly) in the ethane bridge configurations. The two possible skew conformations have been identified by their distinct hydrogen atom locations. The average position of every other atom has been determined.

II crystallizes in the monoclinic space group $P2_1/c$ with four molecules per unit cell of dimensions a = 10.607 (3) Å, b = 26.881 (8) Å, c = 9.499 (2) Å, and β = 115.87 (2)°. The structure has been refined to a conventional R factor of 0.052 for 1979 observable data. There is a similar conformational disorder as for I. However, insufficient resolution prevented the accurate location of each hydrogen atom in the disordered ethane bridge.

The existence of more than one stable molecular conformation in the ground states of [2.2](9,10)anthracenophane and [2.3](9,10)anthracenophane has been shown in another paper[3] and earlier work,[4] so it seemed essential to have an independent model for the assessment of the probable conformations for I and II and their molecular geometries. We have found molecular mechanics calculations to be particularly useful in this regard and we have employed them with considerable success to predict the various conformations of the anthracenophanes and their respective photoisomers.

A general feature of the molecular force field calculations for [2.*n*](9,10)anthracenophanes (*n* = 2–5) is the predicted existence of pairs of conformers. Compared with a hypothetical structure in which the two anthracene fragments would have an eclipsed conformation, one member displays a small relative rotation of the anthracene framework about the interchromophore axis while the other shows a small relative translation parallel to the long molecular axis. The number of pairs is determined by the number of possible conformations of the *n* carbon atom bridge (as constrained by the 1,2-di(9-anthryl)-ethane framework).

The force-field calculations have made possible a rationalization of the spectroscopic and photochemical properties of the [2.*n*](9,10)anthracenophanes. The present paper deals with

0002-7863/80/1502-3524$01.00/0

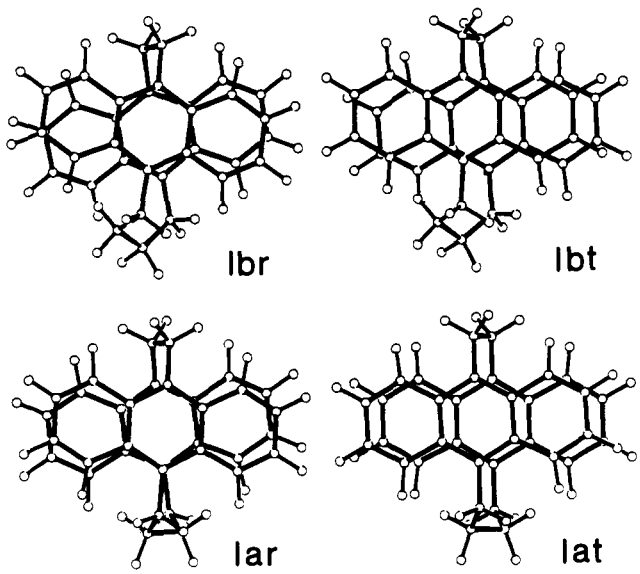

Figure 1. Calculated molecular projections of conformations Iar, Iat, Ibr, and Ibt onto a plane normal to the interchromophore axis.

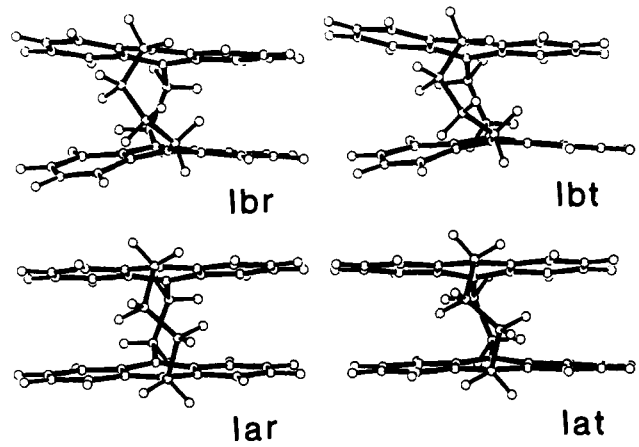

Figure 2. Same as for Figure 1 but onto a plane normal to the mean chromophore short axis.

the compounds I (n = 4) and II (n = 5). Another paper deals with n = 2 and 3.[3]

Experimental Section

Fluorescence spectra were measured with a Spex 1704 monochromator and a RCA C31034 cooled photomultiplier. Excitation was by means of a high-pressure xenon lamp with the light dispersed through a Spex 1402 double monochromator.

The measurement of fluorescence polarization ratio in rigid glasses has been given elsewhere.[5] The same arrangement was used to measure fluorescence quantum yields and calibration, at room temperature, was with 9,10-diphenylanthracene (fluorescence yield 0.86). Control of temperature was by way of cold nitrogen gas in a gas flow tube. Spectroscopic solvents were methylcyclohexane and decalin (1:1, MCH-D) and methylcyclohexane and isopentane (1:3, MCH-IP).

1,4-Di(9-anthryl)butane. To the Grignard reagent prepared from Mg (0.5 g) and 1,4-dibromobutane (1 mL) in anhydrous Et_2O (15 mL), a hot solution of anthrone (2 g, 62% of theoretical amount) in anhydrous benzene (40 mL) was added. The reaction mixture was stirred and refluxed under N_2 for about 20 min, until the color was green. After cooling and decomposition with ice and dilute HCl, the solvents were evaporated and the remainder was washed exhaustively with hot 20% NaOH solution to remove unreacted anthrone. The crude material was washed with H_2O, dried, and crystallized from $CHCl_3$, yield 1.07 g (51%) of nearly colorless prisms, mp 254 °C. Byproducts were anthracene, anthraquinone, and 1,8-di(9-anthryl)-octane.

1,4-Di[9-(10-chloromethyl)anthryl]butane. Pulverized 1,4-di(9-anthryl)butane (0.5 g) and paraformaldehyde (0.5 g) were suspended in dioxane (10 mL) and concentrated HCl (4 mL). The mixture was stirred and refluxed for about 2 h, while a fine stream of HCl gas was passing through. The reaction mixture was kept overnight at room temperature, filtered, and washed with EtOH, ether, and $CHCl_3$, yield 0.44 g (72%) of yellow, crystalline powder, mp > 240 °C dec. Product was used for cyclization without further purification.

[2.4](9,10)Anthracenophane. Dry 1,4-di[9-(10-chloromethyl)-anthryl]butane (200 mg) was suspended in THF (10 mL) and 0.6 M ether solution of PhLi (10 mL) was added. The mixture was stirred and gradually heated until the solution became clear and green-yellow, about 20 min. The reaction was then stopped by addition of excess ice water. After acidification with dilute HCl and evaporation of the solvents over steam, the remainder was washed with H_2O, dried, and chromatographed on a silica gel column using benzene-n-hexane (1:1) as solvent. The second yellow fraction diffused on the large volume of the column was collected, the solvent evaporated, and the residual refluxed for 1 min in the minimum amount of chlorobenzene. A small quantity of petroleum ether (100–130 °C) was added and the solution allowed to crystallize in the refrigerator, yield 17 mg (10%) of yellow prisms, mp > 335 °C dec. Main byproducts were polymers and biphenyl. ^{1}H NMR (bromobenzene-d_5) δ (ppm) 1.22–1.64 (m, 4, internal H of butylene bridge), 2.7–3.2 (m, 4, external H of butylene bridge), 4.06 (s, 4, ethylene bridge H), 6.58–7.09 (m, 8, aromatic H), 7.28–7.56 (m, 4, aromatic H), 7.62–7.86 (m, 4, aromatic H); mass spectrum m/e 436, 204, 191. Anal. ($C_{34}H_{28}$) C, H.

1,5-Di(9-anthryl)pentane was prepared via the Grignard reaction between 1,5-dibromopentane and anthrone as in the synthesis of 1,4-di(9-anthryl)butane, yield 30% of slightly yellow needles, recrystallized from $CHCl_3$–Et_2O, mp 184–185 °C. The main byproducts were 9-pentylanthracene, mp 80 °C, anthracene, and anthraquinone.

1,5-Di[9-(10-chloromethyl)anthryl]pentane. Pulverized 1,5-di(9-anthryl)pentane (0.5 g) and paraformaldehyde (0.5 g) were suspended in dioxane (10 mL) and concentrated HCl (4 mL). The mixture was stirred and a fine stream of HCl gas was bubbled through the mixture for 1 h with the temperature held at 30–40 °C. The reaction mixture was kept for another 1 h at room temperature without passing HCl gas, filtered, washed with EtOH and ether, and dried, yield 0.41 g (67%), mp >220 °C dec.

[2.5](9,10)Anthracenophane. Dry 1,5-di[9-(10-chloromethyl)-anthryl]pentane (200 mg) was suspended in THF (10 mL) and 0.6 M ether solution of PhLi (10 mL) was added. The mixture was stirred and kept at 40 °C until dark green (10–15 min). The excess ice water was added and the isolation of product carried out as for butane analogue, yield 8 mg (5%) of green, fluorescent prisms, mp 320 °C dec. Main byproducts were polymers, biphenyl, and 1,5-di[9-(10-benzyl)anthryl]pentane, mp 255–257 °C. Scaling was unsuccessful. ^{1}H NMR ($CDCl_3$): δ 4.48 (prominent s, 4, ethylene bridge H); mass spectrum m/e 450, 204, 191. Anal. ($C_{35}H_{30}$) C, H.

Empirical Force Field Calculations

The calculations were performed using the force field program MMPI[6] with a modified parameterization.[7] In each case the geometry was fully optimized to provide energy minimization to within 0.005 kcal mol^{-1}.

Compound I. The degrees of freedom of the butane bridge are restricted by its attached 1,2-di(9-anthryl)ethane framework. Trial structures were obtained by considering the butane bridge as a fragment in a virtual cyclohexane ring (C(10) ··· C(10′) virtual bond) and the various conformations were derived accordingly.[8] After geometry optimization, four separate conformers were predicted. We refer to these as Iar, Iat, Ibr, and Ibt, where a and b denote the two different conformations of the butane bridge, while r and t refer to the rotated and translated conformations of the chromophores, respectively. Iar and Iat have C_2 symmetry.

For comparison purposes the computer program[9] generated projections of the structure of each conformer on a plane normal to two of three orthogonal axes are shown in Figures 1 and 2. Some essential nomenclature is defined in Figure 3, while calculated heats of formation, together with relevant geometric parameters for each conformer, are listed in Table

Table I. Force Field Calculations Results: Heat of Formation and Geometry

	$\Delta H_f°$(g), kcal mol^{-1}	contact/bond distance, nm C(9)···C(9′) C(9)-C(9′)	contact/bond distance, nm C(10)···C(10′) C(10)-C(10′)	dihedral angle, deg[a] 1-2	3-4	1-3	2-4
Iar	126.8	0.2741	0.3689	2.4	2.4	14.9	14.9
at	127.6	0.2739	0.3626	3.8	3.8	13.0	13.0
br	131.5	02714	0.3391	16.6	7.8	7.8	28.3
bt	134.0	0.2730	0.3425	16.7	9.1	10.4	28.6
IPa	164.1	0.1680	0.1631	36.6	36.6	40.5	40.6
b	164.5	0.1655	0.1651	54.8	46.2	46.9	54.5
IIar	120.1	0.2771	0.4155	1.6	3.4	20.5	20.5
at	121.4	0.2772	0.4131	5.9	3.6	16.9	24.2
br	121.2	0.2834	0.4492	10.7	5.9	20.4	36.0
bt	121.3	0.2843	0.4531	9.5	7.1	20.9	36.7
cr	121.9	0.2737	0.3896	1.4	1.4	19.9	19.9
ct	123.7	0.2743	0.3875	3.4	3.4	19.4	19.4
IIPa	170.1	0.1676	0.1640	46.1	31.5	41.5	41.7
b	169.7	0.1661	0.1640	42.0	48.4	42.3	51.9
c	165.1	0.1667	0.1641	41.0	41.0	43.6	43.6

[a] See Figure 3.

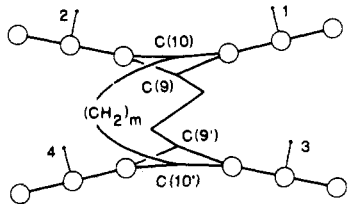

Figure 3. Definition of the dihedral angles: 1, 2, 3, and 4 are the normals to the best planes through the carbon skeletons of each benzene ring. Typical deviations of the carbon atoms from the best plane are up to 0.005 nm for I or II and up to 0.008 nm for their photoisomers.

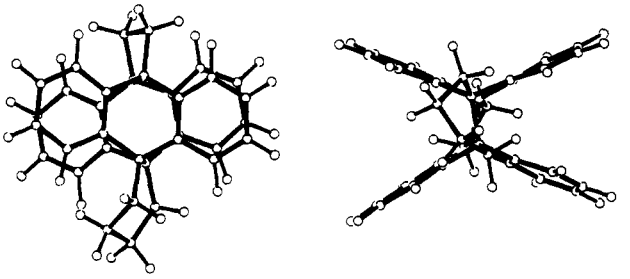

Figure 5. Calculated molecular projections for the photoisomer IPb.

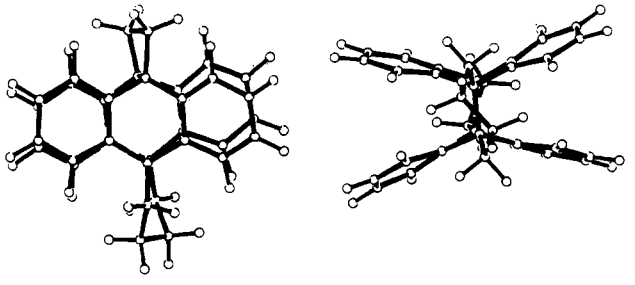

Figure 4. Calculated molecular projections for the photoisomer IPa.

I. As there are no experimental measurements of heats of formation, the error in the calculated enthalpies of formation in the gas phase, $\Delta H_f°$(g), can only be estimated. In view of the molecular size and the type of strain involved, an error of several kilocalories per mole seems likely. However, this error should be constant for the various conformations of one molecule, so that the relative order of calculated energies is probably a true indication of relative stability. Hence the predicted, most stable, conformations Iar and Iat (in the gas phase) correspond precisely to the observed structure (in the condensed phase). The conformations of the butane bridge in Iar and Iat are very similar to that observed, with a mean deviation in the C-C-C-C torsional angles of less than 4°. Moreover, Iar and Iat are basically different, each having the "opposite" skew conformation of the ethane bridge (Figure 2), as observed.

Molecules of either Iar and Iat conformation randomly occupy any one site in the crystal. The X-ray analysis indicates that the positions occupied by atoms C(9′), C(10), and C(10′) of both conformers almost coincide in the crystal lattice. Therefore, distances between these (averaged) atoms, derived from the X-ray experiment, will approximate closely the corresponding distances in the separate conformers. It follows, in particular, that the C(10)···C(10′) contact distance provides a useful comparative yardstick between theory and experiment. Calculated C(10)···C(10′) distances for Iar and for Iat are 0.369 and 0.363 nm, respectively, compared with the "observed" distance of 0.3874 (3) nm. Given the complexity of the molecule, and the fact that the calculations take no account of crystal packing effects, this measure of agreement ($\Delta \approx 0.02$ nm) seems satisfactory. The C(9)···C(9′) contact distance is less well defined experimentally, but the "observed" value 0.2797 (3) nm again compares favorably with those derived from the force-field calculations (av 0.274 nm for Iar and Ibr). The anthryl chromophores are slightly distorted from planarity by folding and twisting (see Figures 1 and 2). The angles between the outer benzene rings are 177.6 and 176.2° in Iar and Iat, respectively.

Compound I Photoisomer. The molecular force field program was used also to calculate possible structures for the photoisomer of I. Two possibilities were found (IPa and IPb; Figures 4 and 5). Their predicted geometries and heats of formation are included in Table I. It is somewhat surprising that the calculations predict the two photoisomers to have very similar enthalpies, whereas their structural geometries are strikingly different. The calculated enthalpies of formation of the photoisomers are probably less reliable than those of the more usual isomers because of the difficulty of assigning some of the bond and structure energies.[7] This applies in particular to the elongated C(9)-C(9′) and C(10)-C(10′) bonds. However, as these terms depend only on the atom group and bond types involved, the relative stability should be predicted correctly, although the estimated enthalpy of the photoisomerization reactions bears a (constant) error.

Compound II. Trial structures have been derived by considering the pentane bridge as a fragment in a virtual cycloheptane ring (C(10)···C(10′) virtual bond), with known possible conformations.[10] Calculations predict six stable

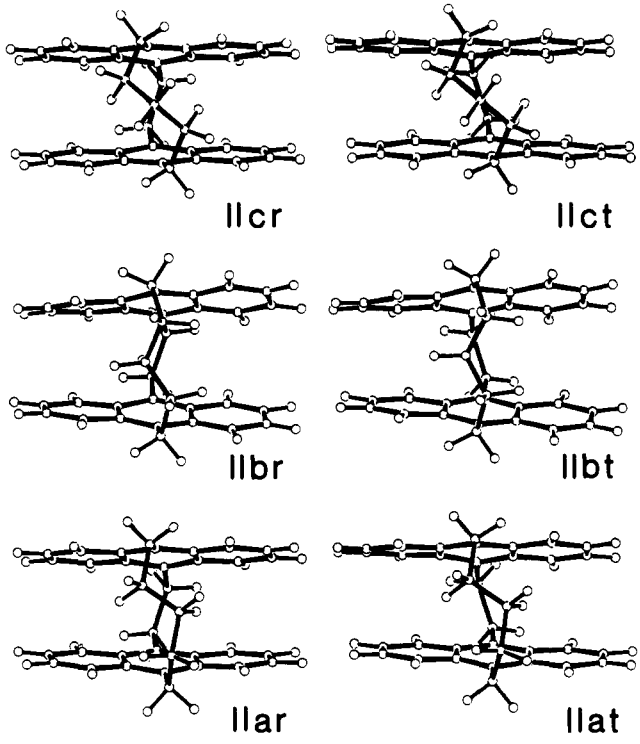

Figure 6. Calculated molecular projections of the conformations IIar, IIbr, IIcr, IIat, IIbt, and IIct onto a plane normal to the mean chromophore short axis.

conformations (IIar, IIat, IIbr, IIbt, IIcr, and IIct). Their heats of formation and relevant geometric parameters are also detailed in Table I. One set of molecular projections for each conformer is given in Figure 6.

By inspection of the torsional angles in the pentane bridge, the structure of II in the crystal can be readily identified as corresponding to a superposition of IIbr and IIbt conformations alone. The mean deviations between the experimental and calculated C-C-C-C torsional angles are 9 and 5°, respectively, while mean deviations exceeding 23° were found for the other calculated conformers. The locations of the central atoms, C(9), C(9′), C(10), and C(10′), are not greatly affected by the crystal disorder, so that a comparison between the calculated and observed C(9) ··· C(9′) and C(10) ··· C(10′) contact distances can be made. The calculated values are 0.283 and 0.449 nm, respectively, in IIbr and 0.284 and 0.453 nm, respectively, in IIbt, in reasonable agreement with the experimental values of 0.2900 (5) and 0.4647 (5) nm. Meanwhile, corresponding values in the other conformers are significantly shorter; in particular the C(10) ··· C(10′) distances are 0.414 nm in IIar and IIat and 0.389 nm in IIcr and IIct.

Whereas little significant difference between the calculated enthalpies of formation of the various conformers of II was found, only two conformations were found in the condensed phase. They have the largest interchromophore separation.

Compound II Photoisomer. Three possible photoisomers are predicted. The most stable, IIPc, shows no evidence of unusual strain (cf. other anthracenophane photoisomers) apart from a succession of four widely bent C-C-C bond angles (120°) in the cycloheptane ring. However, we were unable to observe photochemical activity and no photoisomer could be obtained. The molecular projections of IIPc are given in Figure 7.

Fluorescence and Photochemistry of I. We expected to observe a viscosity- and temperature-dependent variation of the fluorescence yield, as is common for 9-substituted anthracenes.[11] However, the behavior we found is more complex than was observed for 1-(9-anthryl)-3-(1-naphthyl)propane.[12] In both solvents (MCH-D and MCH-IP) the yields approached

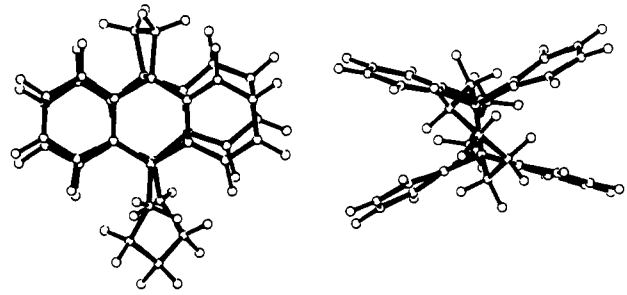

Figure 7. Calculated molecular projections for the photoisomer IIPc.

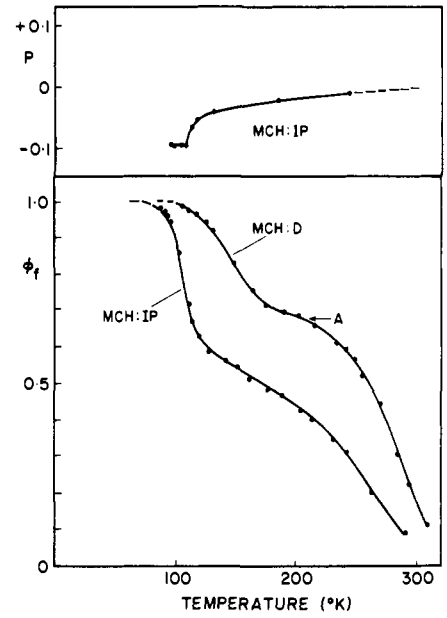

Figure 8. Lower: fluorescence yield of I as a function of temperature in two glassy solvents, methylcyclohexane–isopentane (1:3) (MCH-IP) and methylcyclohexane–decalin (1:1) (MCH-D). Upper: polarization of fluorescence (P) as a function of temperature in MCH-IP.

unity as the temperature was lowered and the results are shown in Figure 8.

Considering the results for I in MCH-IP, we note that the yield drops rapidly between 100 and 120 K. Measurements of the temperature dependence of the fluorescence polarization ratio (P), included in Figure 8, show that rotational depolarization sets in at about 110 K, so that the fluorescence quenching does not bear a simple one to one correspondence with rotational relaxation during the excited state.

In MCH-D the analogous quenching of the fluorescence occurs at higher temperatures and over a larger temperature range, so it seems likely that the solvent viscosity is the controlling factor.

The clue to the interpretation of the temperature-dependent quenching is provided by measurements of the fluorescence spectra as a function of temperature. A series of spectra of I in MCH-D are given in Figure 9. These spectra show that, as the temperature is raised from about 100 K to just below about 200 K, the spectral distribution of the fluorescence intensity shifts progressively to lower energy by about 600 cm^{-1}. In addition, the spectral bandwidth increases and the band becomes more asymmetrical in its intensity distribution toward the low-energy side of the maximum. These changes must arise from a relaxation, during the lifetime of the excited state, whereby the two chromophores approach each other more closely.

The absorption spectrum of I in MCH-D, at about 100 K, has an intensity distribution which corresponds to the conformation Iar, not Iat, previous work[3] having established the

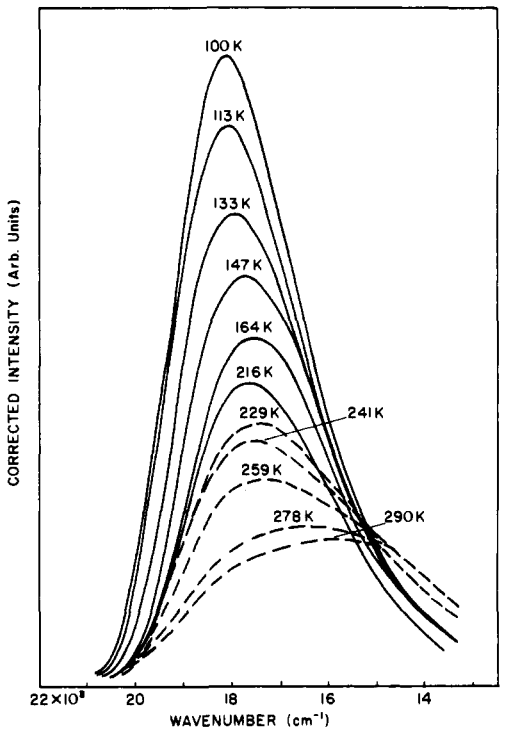

Figure 9. Fluorescence spectra of 1 measured in MCH-D at various temperatures.

spectral differences between rotated and translated conformations of the anthracene chromophores. Absorption of light carries the molecule to an excited state in which the electronic excitation energy is delocalized between the two chromophores. The molecule can now minimize its electronic energy through a closer approach of the two chromophores, thereby reaching a more stable excimer configuration.

Following this there will be a relaxation to the conformation which is related to the ground-state conformation Iat. We see from Figures 1 and 2 that in order to achieve this change there must be a relative translation of one anthryl chromophore over the other which brings also a change of conformation of the ethane bridge. These changes will be inhibited by the viscosity of the solvent because there must be associated adjustments of the solvent molecular cage. They can also occur while the local viscosity is too high to allow appreciable molecular rotation during the lifetime of the excited state. This is in agreement with our experimental results in Figure 8.

The change of fluorescence yield in the temperature range below about 200 K and the associated small shift of the fluorescence band maximum are therefore very probably a consequence of a relaxation of the excited molecule from the ground-state rotated chromophore conformation to a translated conformation, which allows a slightly closer approach of the two chromophores without a major change of conformation of the butane bridge.

It is useful to carry out a quantitative analysis of the temperature dependence of the fluorescence yield using a simple model. The fluorescence rate is denoted by k_f and a thermally activated first-order quenching rate denoted by

$$k_q = A \exp(-E/RT)$$

The fluorescence yield is therefore given by

$$\phi_f = k_f/(k_f + k_q) \qquad (1)$$

It follows that

$$\ln (\phi_f^{-1} - 1) = \ln (A/k_f) - E/RT \qquad (2)$$

The data in Figure 8 are plotted in this way in Figure 10.

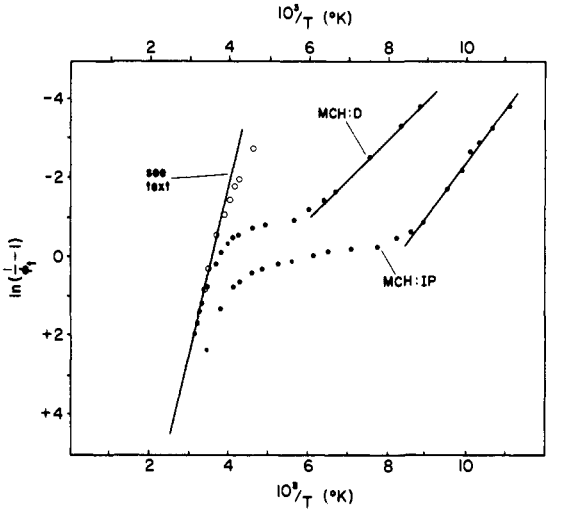

Figure 10. Arrhenius plots of the fluorescence yield data of Figure 8.

Presented in this form, the effect of the solvent viscosity on the fluorescence yield is more easily seen. For MCH-D, ln (A/k_f) = 5.0 and E = 2.0 kcal mol^{-1}. The corresponding parameters in MCH-IP are 11.2 and 2.6 kcal mol^{-1}. The essential difference is therefore in the frequency factor, which is 500 times larger in MCH-IP.

From Figure 8 we also see that the higher temperature quenching region sets in at about the same temperature for both solvents and the quenching is probably an intrinsic molecular process.

From Figure 9 we see that there is a very marked difference in the spectral distributions of the spectra observed at 229 K and above and the 216 K spectrum. The higher temperature spectra show a pronounced increase in the intensity of the low-energy regions < 16 000 cm^{-1}. Subtraction of the 216 K band shape from the 241 K spectrum revealed a broad band with maximum at about 14 000 cm^{-1}. The onset of the new region of fluorescence quenching coincides, therefore, with the appearance of a new fluorescence band. Further understanding requires a determination of the temperature dependence of the fluorescence decay time, which is given in Figure 11.

Analysis of the high-temperature quenching region in the decay times was made using the following Arrhenius equation:

$$\ln (1/\tau - 1/\tau_0) = \ln A - E/RT$$

τ_0 was taken to be 63.0 ns (see Figure 4) and the resulting plot is also given in Figure 11. The very good linear relation provides the parameter values E = 8.3 kcal mol^{-1} and A = 4.6 × 10^{13}.

If we take these parameters and put $k_f = 1/\tau_0 = 1.6 \times 10^7$ s^{-1}, we can calculate the equivalent Arrhenius relation in (2). This calculated line is shown in Figure 10 and the observed values of ln $(\phi_f^{-1} - 1)$ are seen to lie below this line, indicating that the values of ϕ_f are too small. If we calculate a new set of ϕ_f's normalized to the original ϕ_f = 0.68 as unity (shown by A in Figure 8), then the new set of values of ln $(\phi_f^{-1} - 1)$ are shown by the open circles in Figure 10. The agreement between these new values and the calculated line is very good, thus bringing the decay-time measurements into complete agreement with the fluorescence yield results.

A consistent picture emerges. Absorption of light by a molecule carries it to the excited state. The equilibrium conformation of this state is not the same as that of the ground state and relaxation to the new geometry takes place, subject to possible constraints by the solvent cage. This new conformation has the two chromophores slightly closer together, because the fluorescence spectrum is shifted by 600 cm^{-1} to

lower energy. The extent to which this change can be effected, during the lifetime of the excited state, depends on the solvent viscosity. The new conformation has a fluorescence yield of 0.68 and a lifetime of 63 ns in MCH-D. Further increase of temperature has little effect on these parameters until a new quenching process starts at about 200 K. This must involve a major conformational change in the molecule as there is a shift of the fluorescence band maximum from 17 600 to 14 500 cm^{-1}. Such a large shift is indicative of a larger interaction between the chromophores, which means a relaxation into another conformation, with the chromophores closer together than in the primary relaxed conformation (related to the ground-state conformation Iat). This brings us to a consideration of conformations Ibr and Ibt.

The enthalpies of formation of Ibr and Ibt are 131.5 and 134.0 kcal mol^{-1}, about 4 and 7 kcal mol^{-1}, respectively, higher than those of Iar and Iat. The important difference between the a and b conformers comes from the changed conformation of the butane bridges and is reflected in significant differences in the C(10) · · · C(10′) contact distances. In Ibr and Ibt, the C(10) · · · C(10′) distance is 0.025 nm shorter than in Iar and Iat.

Relaxation of the excited molecule from the Iat related conformation into either the related Ibr or Ibt conformations must involve an activation barrier, because of the conformational change in the butane bridge. The Arrhenius plot in Figure 10 provides a barrier of 8.3 kcal mol^{-1}, a reasonable value.

As the primary relaxation is to the excited conformation related to Iat, we expect that the activated secondary relaxation will be to a conformation which is related to the Ibt conformation. A final relaxation should then occur to the excited-state analogue of Ibr which is calculated to have a still shorter C(10) · · · C(10′) distance. The fluorescence, with band maximum at 14 500 cm^{-1}, is therefore probably from this final relaxed conformation. The fluorescence is in competition with photoisomerization, so we expect that the photoisomer (kinetic product) will have a structure in which the ethane and butane bridges have conformations closely related to those of the conformer Ibr; i.e., it should be IPb rather than IPa (see Figures 4 and 5).

It is not possible to make a comparison with experiment, because the molecular structure of the photoisomer is not known. It is so thermally unstable that low-temperature X-ray structure data are required and these have not so far been obtained. However, the crystal structure of the photoisomer of 1,4-di(9-anthryl)butane[13] has been determined and the cyclohexane ring has the same distorted boat conformation as in Ibr.

It should be noted in relation to the activation barrier, that the transition to the boat-like conformation of the butane bridge requires a large bending of the C-C-C bond angles. One of these reaches 126.4° for Ibt (124.6° for Ibr). This strain is somewhat reduced in the cyclohexane ring of the photoisomer where the C-C-C bond angles range from 108.7 to 112.7°, except for one which is 122.6°. This is to be compared with the observed value of 120.1° in the molecular structure of the photoisomer of 1,4-di(9-anthryl)butane.[13]

The molecular force field calculations have provided two photoisomer structures with very similar enthalpies. Emphasis has been given to one of these (IPb) by analogy with the known structure of the 1,4-di(9-anthryl)butane photoisomer.[13] However, no other evidence was found from conformational analysis which argues against the formation of IPa. It is likely that an equilibrium between IPb and IPa is quickly established and both are present in solution, although IPb might be found in the crystal.

Fluorescence of II. The characteristics of the fluorescence of II were determined in MCH-D and the temperature dependence of the quantum yield is shown in Figure 12. Measurements of the fluorescence intensity distribution revealed distinct quantitative differences in the excited-state behavior of this molecule compared with those of I.

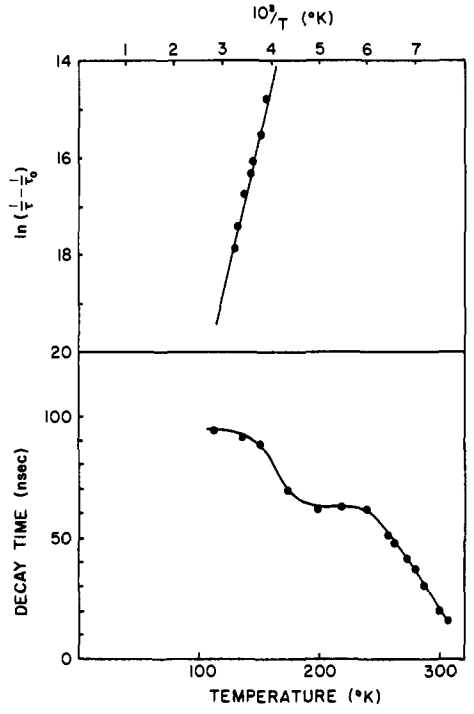

Figure 11. Lower: decay times of I measured at various temperatures in MCH-D. Upper: Arrhenius plot of the decay-time data.

To begin with, the fluorescence spectra in Figure 13 show that, on raising the temperature from 122 to 140 K, there is a shift of the position of the maximum intensity to lower energy by about 600 cm^{-1}. However, the fluorescence yield remains constant at unity (Figure 12), which is also consistent with the observation of an isolampsic point (see arrow in Figure 13). The small shift of the intensity maximum to lower energy and the change of band shape are indications that relaxation brings the two chromophores slightly together.

Above about 140 K the fluorescence yield is reduced by the onset of some quenching mechanism and there is a small shift of about 500 cm^{-1} to lower energy between 140 and 210 K. Further increase of temperature leads to a more rapid reduction in the fluorescence yield and the fluorescence maximum shifts to higher energy. An Arrhenius plot (eq 2) of the data in Figure 12 shows that the fluorescence quenching region between 140 and about 200 K has an activation barrier of 2.2 kcal mol^{-1} and $\ln(A/k_f) = 4.6$, very similar to the analogous parameters for I.

Unlike the result for I, there is no appearance of a lower energy fluorescence band with increasing temperature. Instead, the band maximum shifts to higher energy as the temperature is raised above about 210 K. An Arrhenius plot provided a barrier of 4.4 kcal mol^{-1} and $\ln(A/k_f) = 8.8$.

The fluorescence band maximum should show a good qualitative correlation with C(10) · · · C(10′) atom contact, insofar as the latter is a measure of the mean interchromophore separation. A decrease of this separation increases overlap, so that the band maximum moves to lower wavenumber. The molecular conformations IIbr and IIbt have the longest C(10) · · · C(10′) atom distances and they are the most favored candidates for the ground state, at least in the crystalline form. We assume that the same holds true in the solvents used in the present work. The 100 K absorption spectrum is consistent with the IIbr conformation.

The temperature dependence of the fluorescence between

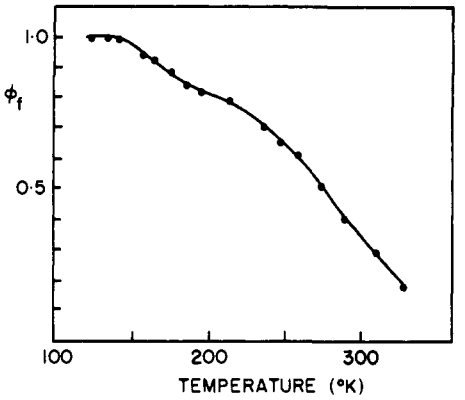

Figure 12. Fluorescence yield of II as a function of temperature in MCH-D.

122 and about 140 K showed no change of fluorescence yield, but there was a small shift of the band maximum to lower wavenumber. We interpret these results in the following way. After the absorption of light, the molecule retains the same conformation as it had in the ground state (IIbr), but the chromophores relax slightly by reducing the interchromophore separation. This relaxation is controlled by temperature through the local viscosity, but there is no change of yield because the same molecular conformation is involved. Above about 140 K, there appears a thermally activated process which brings a lowering of the yield and a shift of the band maximum to lower wavenumber. This shift is indicative of a decrease of the interchromophore separation toward another conformation which has a lower yield. The activation barrier (2.2 kcal mol^{-1}) and frequency factor ($\ln (A/k_f) = 4.6$) are very similar to those observed for the corresponding quenching process in I. The activated relaxation then involves a transition to the excited-state analogue of IIbt. The slightly larger barrier and somewhat higher temperature range for this relaxation might very well reflect the greater involvement of solvent molecules because of the more open "mouth" of II.

Contrary to the behavior observed for I, above about 210 K the fluorescence band maximum shifts to higher energy and there is no growth of a lower energy band as was observed for I. This indicates a thermal population of the two excited conformations related to IIbr and IIbt. An estimate of the energy difference between the two conformations in the solvent is provided by the difference between the activation barriers for the forward and backward paths i.e., 2.2 kcal mol^{-1}.

The reason for the nonappearance of a red-shifted fluorescence band at higher temperature must be related to the absence of a photoisomer. The molecular force field calculations

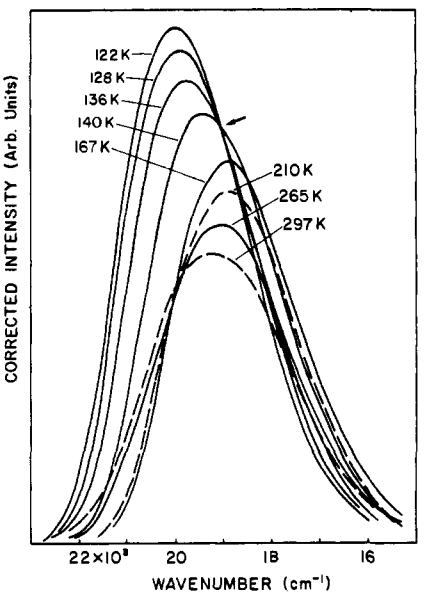

Figure 13. Fluorescence spectra of II measured in MCH-D at various temperatures.

showed that the most likely conformation of the photoisomer will have the c conformation of the pentane bridge similar to that in IIcr. The transition from IIbt to IIcr requires two internal rotations of the pentane bridge, presumably through IIar and/or IIat. The barriers to these rotations could very well be much too high to provide a measurable rate during the lifetime of the excited state. The absence of a photoisomer and the absence of a red-shifted fluorescence band are both compatible with the absence of conformations related to either IIcr or IIct as relaxed forms in the excited state of the molecule.

References and Notes

(1) Wada, A.; Tanaka, J. *Acta Crystallogr., Sect. B* **1977**, *33*, 355.
(2) Dunand, A.; Robertson, G. B., to be published.
(3) Dunand, A.; Ferguson, J.; Puza, M.; Robertson, G. B. submitted for publication in *Chem. Phys.*
(4) Ferguson, J.; Morita, M.; Puza, M. *Chem. Phys. Lett.* **1977**, *49*, 265.
(5) Ferguson, J.; Mau, A. W-H.; Whimp, P. O. *J. Am. Chem. Soc.* **1979**, 101, 2363.
(6) Kao, J.; Allinger, N. L. *J. Am. Chem. Soc.* **1977**, *99*, 975.
(7) Dunand, A., submitted for publication in *Chem. Phys.*
(8) Dunitz, J. D. *J. Chem. Educ.* **1970**, *47*, 488.
(9) Johnson, C. K. ORTEP Report ORNL-5138, Oak Ridge National Laboratory, Oak Ridge, Tenn., 1976.
(10) Bocian, D. F.; Pickett, H. M.; Rounds, T. C.; Strauss, H. L. *J. Am. Chem. Soc.* **1975**, *97*, 687.
(11) Bowen, E. J.; Sahu, J. *J. Phys. Chem.* **1959**, *63*, 4.
(12) Ferguson, J.; Mau, A. W-H.; Whimp, P. O. *J. Am. Chem. Soc.* **1979**, *101*, 2370.
(13) Dunand, A.; Robertson, G. B., to be published.